Electronic Supplementary Material (ESI) for:

Trinary Support of Ni/NiO/C to Immobilize Ir Nanoclusters for Alkaline Hydrogen Oxidation

Ziliang Kang,[a] Yao Peng,[a] Zi Wei,[a] Yuanjun Liu, *[b] Xiaoyang Song,[a] Zhenyuan Ji,[a] Xiaoping Shen,[a] Ning Yao,[a] Xinhang Du,[a] Guoxing Zhu*[a]

[a]School of Chemistry and Chemical Engineering, Jiangsu University, Zhenjiang, China,

Email: zhuguoxing@ujs.edu.cn

[b]School of Environmental and Chemical Engineering, Jiangsu University of Science and Technology, Zhenjiang 202018, China, Email: liuyuanjun@just.edu.cn

Characterization

X-ray powder diffraction (XRD) analysis was recorded by using a Rigaku Miniflex 600 device equipped with copper Kα radiation source (λ = 0.154178 nm), which was performed within 2θ range from 20° to 80° with a scanning rate of 10° min^{-1}. The morphology and microstructure of the sample were visualized using a FEI Quanta 200F scanning electron microscope (SEM) with an accelerated voltage of 20 kV. For transmission electron microscopy (TEM) observation, a FEI Tecnai G20 UTwin transmission electron microscope with an acceleration voltage of 200 kV was employed. X-ray photoelectron spectroscopy (XPS) measurements were acquired with a Kratos XSAM 800 spectrophotometer. Additionally, the analysis for inductively coupled plasma atomic emission spectroscopy (ICP-AES) was carried out employing a Thermo IRIS Intrepid II XPS atomic emission spectrometer. Thermogravimetric analysis and differential scanning calorimetry (TG-DSC) are performed using the DZ-STA200 synchronous thermal analyzer.

Electrochemical investigation

Electrochemical tests were performed by using CHI730E electrochemistry workstation. A Hg/Hg_2Cl_2 electrode filled with 0.1 M KOH was employed as the reference electrode. The counter electrode utilized is a graphite rod with a diameter of 4 mm. The employed working electrode is a glass carbon (GC) rotating disk electrode with a diameter of 4 mm, which was modified by the catalyst. To prepare the catalyst ink, combine 4.0 mg of catalyst with 960 μL of ethanol and 40 μL of 5 $_{wt}$% Nafion solution. The resulting mixture was subjected to ultrasonication for 30 minutes to achieve a homogeneous catalyst ink. 10 μL of the catalyst ink was applied onto the working electrode to provide catalyst mass loading of 0.318 mg cm_{disk}^{-2}. To ensure consistency, all measured potentials

were converted to values referenced to the reversible hydrogen electrode (RHE). No iR compensation was implemented.

Cyclic voltammetry (CV) test was conducted initially in an Ar-saturated 0.1 M KOH aqueous solution, spanning a potential range of -0.05 to 1.05 V (*vs* RHE) to acquire a stable current-potential curve. Subsequently, polarization curves were obtained in an H_2-saturated electrolyte through rotating disk electrode (RDE) immersed, which with a rotation speed of 1600 rpm and a scanning rate of 5 $mV \cdot s^{-1}$.

Supplementary methods

Supplementary methods HOR polarization curves at different rotating rates (400, 900, 1600, 2500 and 3600 rpm) were conducted to extract the kinetic current density (j^k) of each catalyst from the Koutecky-Levich equation (Eq. 1) [S1-S3],

$$\frac{1}{j} = \frac{1}{j^k} + \frac{1}{j^d} = \frac{1}{j^k} + \frac{1}{BC_0\omega^{1/2}} \quad \text{..... Eq. 1}$$

where j is the measured current density, j^d is the diffusion limited current density, B is the Levich constant, C_0 is the solubility of H_2 (7.33×10^{-4} mol L-1), ω is the rotating speed, respectively. Among them, B could be calculated from Eq. 2 [S1-S4],

$$B = 0.62nFD^{2/3}\nu^{-1/6} \quad \text{..... Eq. 2}$$

where n is the electron transfer number, F is the Faraday constant (96485 C mol^{-1}), D is the diffusivity of H_2 (3.7×10^{-5} cm^2 s^{-1}), and ν is the kinematic viscosity (1.01×10^{-2} cm^2 s^{-1}).

Exchange current density (j^0) was deduced from the Butler-Volmer equation (Eq. 3) [S3-S7],

$$j^0 = \frac{RTj}{F\eta} \quad \text{..... Eq. 3}$$

j^0 can be obtained by fitting the kinetic current into the linearized Butler-Volmer equation (Eq. 3), where R is the universal gas constant (8.314 J mol^{-1} K^{-1}), T is the operating temperature (298.15 K), F is the Faraday constant (96485 C mol^{-1}).

Electrochemical active surface areas (ECSAs) were estimated via Cu underpotential deposition (UPD) stripping for all samples after HOR tests. The catalysts were firstly cycled in Ar-saturated 0.1 M H_2SO_4 solution to guarantee a repeatable voltammogram curve as the background, and then were kept at 0.30 V (vs RHE) for 100 s in an Ar-saturated 0.1 M H_2SO_4 solution containing 2 mM $CuSO_4$. UPD Cu oxidation polarization curve was performed from 0.30 to 1.10 V with a scan rate of 10 mV s^{-1}. The ECSAs were calculated via Eq. 4 [S5-S7],

$$ECSA = \frac{Q_{Cu}}{Q_s m_{metal}} \quad \text{..... Eq. 4}$$

where Q_{Cu} stands the measured integral charge, Q_s represents the surface charge density of 420 μC cm_{metal}^{-2} for monolayer adsorption of Cu-UPD stripping, m_{metal} is the mass of the metal on GC.

The calculation methods of $j^{k,m}$, $j^{0,m}$ and $j^{0,s}$ are as follows:

$$j^{k,m} = \frac{j^k}{m_{metal}}$$

$$j^{0,m} = \frac{j^0}{m_{metal}}$$

$$j^{0,s} = \frac{j^{0,m}}{ECSA}$$

Supplementary figures

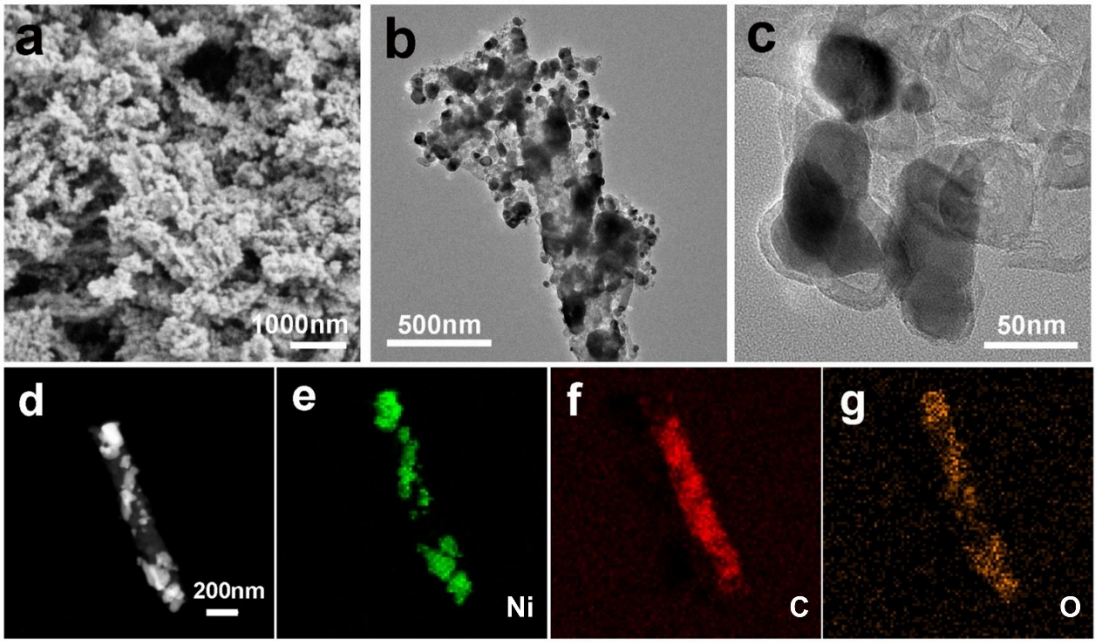

Fig. S1. Microstructure analysis of the Ni/NiO/C product. a) SEM image, b, c) TEM image, d-g) element mapping analysis for Ni, C, and O elements.

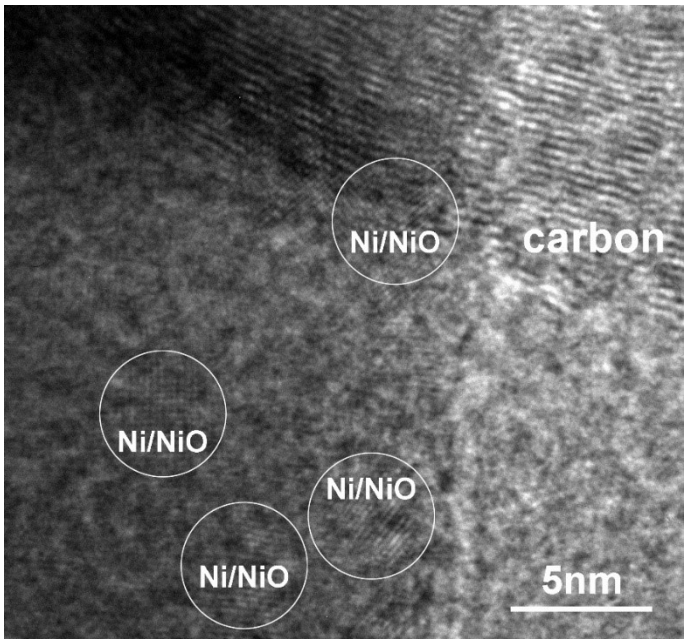

Fig. S2. HRTEM analysis of the Ni/NiO/C product.

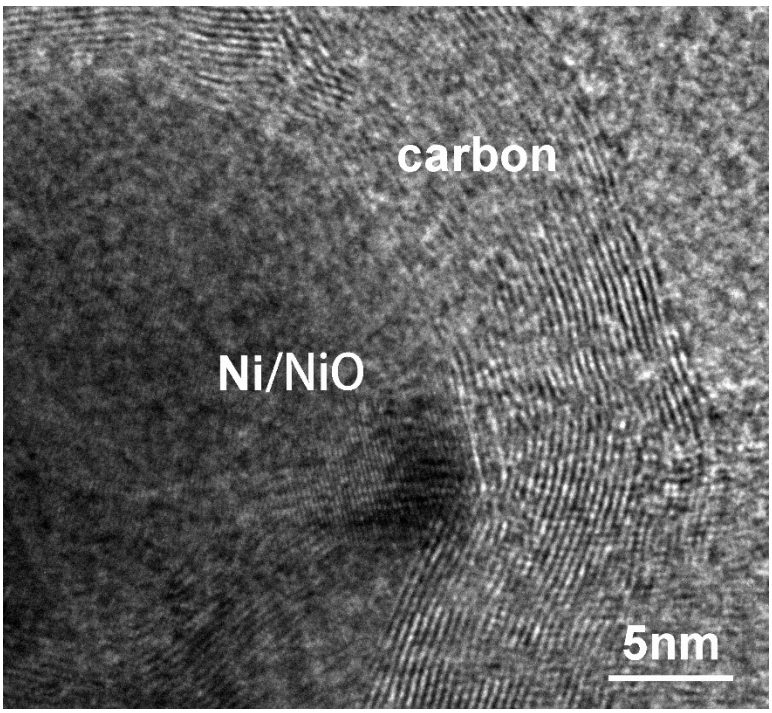

Fig. S3. HRTEM analysis of the Ni/NiO/C product.

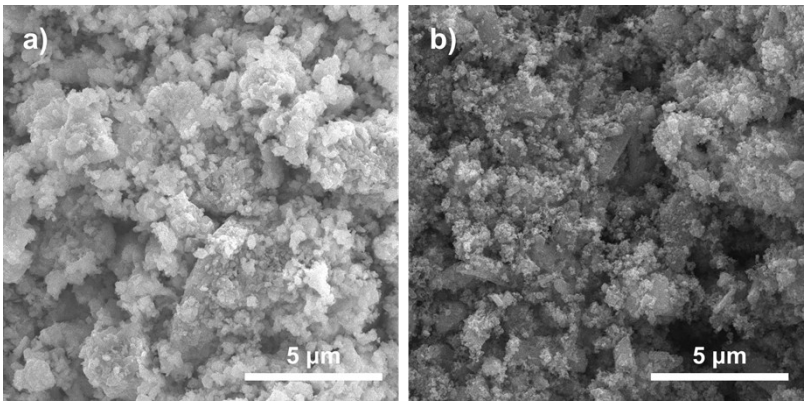

Fig. S4. SEM of the a) Ir-Ni/C and b) Ir-NiO/C product.

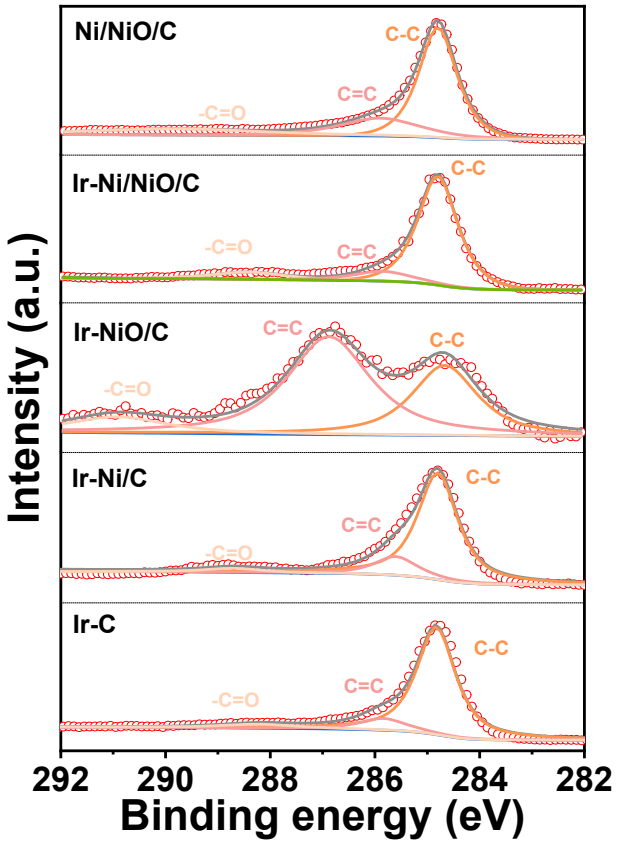

Fig. S5. XPS analysis of the Ir-Ni/NiO/C-3 samples of C.

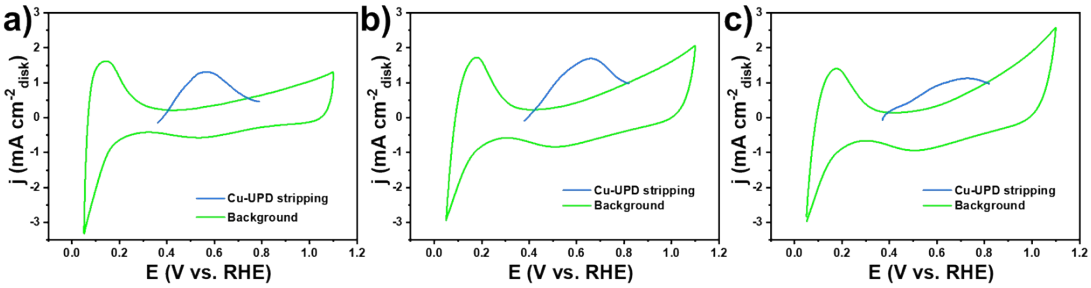

Fig. S6. Cu-UPD stripping voltammograms of a) Ir-Ni/NiO/C-3, b) Pt/C and c) Ir-C. The scan rates are 10 mV s^{-1}.

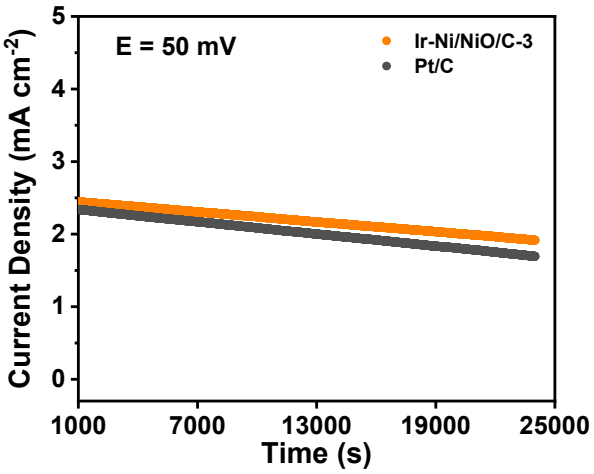

Fig. S7. Chronoamperometry method (i-t) analysis of the Ir-Ni/NiO/C-3 samples and Pt/C.

Supplementary tables

Table S1. ICP-AES data of different materials

Catalysts	Ir (wt%)	Ni (wt%)
Ir-Ni/NiO/C-1	2.99%	45.51%
Ir-Ni/NiO/C-2	5.87%	44.23%
Ir-Ni/NiO/C-3	8.33%	43.10%
Ir-Ni/NiO/C-4	11.91%	42.01%
Ir-Ni/C	10.26%	45.62%
Ir-NiO/C	8.96%	40.94%
Ir-C	19.96%	—

Table S2. Summary of ECSA, j^k, j^0, $j^{k,m}$, $j^{0,m}$, and $j^{0,s}$ of various catalysts.

Catalysts	ECSA ($cm^2\ \mu g_{Ir\ or\ Pt}^{-1}$)	$j^k_{@50mV}$ ($mA\ cm_{disk}^{-2}$)	$j^{k,m}_{@50mV}$ ($mA\ \mu g_{Ir\ or\ Pt}^{-1}$)	j^0 ($mA\ cm_{disk}^{-2}$)	$j^{0,m}$ ($A\ g_{Ir\ or\ Pt}^{-1}$)	$j^{0,s}$ ($\mu A\ cm_{Ir\ or\ Pt}^{-2}$)
Pt/C	0.492	3.176	0.050	1.394	21.886	44.484
Ir-C	0.511	2.028	0.034	1.337	21.033	41.160
Ir-Ni/C	0.239	0.134	0.005	0.093	2.846	11.908
Ir-NiO/C	0.727	1.302	0.052	0.866	30.349	41.746
Ir-Ni/NiO/C-1	0.694	1.576	0.165	0.883	92.730	133.646
Ir-Ni/NiO/C-2	0.622	3.766	0.201	1.625	86.925	139.751
Ir-Ni/NiO/C-3	0.489	3.984	0.151	1.870	70.490	144.151
Ir-Ni/NiO/C-4	0.477	3.342	0.088	1.548	40.812	85.560

Supplementary references

S1. W. C. Sheng, H. A. Gasteiger and S. H. Yang, J. Electrochem. Soc., 2010, **157**, B1529-B1536.

S2. J. Zheng, Z. B. Zhuang, B. J. Xu and Y. S. Yan, ACS Catal., 2015, **5**, 4449-4455.

S3. Y. Yang, X.D. Sun, G.Q. Han, Angew. Chem. Int. Ed,2019, **58**, 10644-10649.

S4. T. Tang, X.Z. Liu, X. Luo, J. Am. Chem. Soc., 2023, **145**, 13805-13815.

S5. X. F. Ji, P. Chen, Y. J. Liu, Z. Y. Ji, H. B. Zhou, C. Y. Chen, X. P. Shen, X. Q. Fu and G. X. Zhu, J. Mater. Chem. A, 2023, **11**, 5076-5082

S6. H. S.Wang, H. D. Abruna, J. Am. Chem. Soc., 2017, **139**, 6807-6810.

S7. D. Liu, S.Q. Lu, Y.R. Xue, Nano Energy, 2019, **59**, 26-32.